

# ATP SYNTHASE — A MARVELLOUS ROTARY ENGINE OF THE CELL

Masasuke Yoshida, Eiro Muneyuki and Toru Hisabori

ATP synthase can be thought of as a complex of two motors — the ATP-driven  $F_1$  motor and the proton-driven  $F_0$  motor — that rotate in opposite directions. The mechanisms by which rotation and catalysis are coupled in the working enzyme are now being unravelled on a molecular scale.

## ELECTROCHEMICAL POTENTIAL GRADIENT

When two aqueous phases are separated by a membrane, the electrochemical potential difference of  $H^+$  between the two phases is expressed as  $\Delta\bar{\mu}_{H^+} = F\Delta\psi - 2.3RT\Delta pH$ , where  $F$  is the Faraday constant,  $\Delta\psi$  is the electric potential difference between two phases,  $R$  is the gas constant,  $T$  is the absolute temperature and  $\Delta pH$  is pH difference between two phases.

“All enzymes are beautiful, but ATP synthase is one of the most beautiful as well as one of the most unusual and important” said Paul Boyer<sup>1</sup>. ATP synthase — also called the  $F_0F_1$ -ATP synthase or  $F_0F_1$ -ATPase — synthesizes cellular ATP from ADP and inorganic phosphate ( $P_i$ ). The energy for ATP synthesis is provided from downhill  $H^+$  (proton) transport along the gradient of ELECTROCHEMICAL POTENTIAL of protons across membranes<sup>2</sup> ( $\Delta\bar{\mu}_{H^+}$ ). This potential is built by the electron-transfer chains of respiration or photosynthesis, which pump protons against a gradient (FIG. 1).

Boyer’s admiration for ATP synthase is justified for two reasons. First, ATP supports nearly all the cellular activities that require energy. ATP synthesis is the most prevalent chemical reaction in the biological world, and ATP synthase is one of the most ubiquitous, abundant proteins on Earth. From *Escherichia coli* to plants and mammals, this enzyme is one of the most conserved during evolution, with >60% of the amino-acid residues of the catalytic  $\beta$ -subunit being conserved<sup>3–5</sup>. Second, ATP synthase uses physical rotation of its own subunits as a step of catalysis — a novel mechanism, different from that of any other known enzyme. Rotation is not a favourite motion in living organisms; there is no animal with wheels, no bird with a propeller and no fish with a screw. On a molecular scale, apart from ATP synthase, only bacterial flagella are known as a rotary motor. The crystal structures of the main part of the ATP synthase show, in atomic detail, how the appearance of this tiny motor made from ~3,500 amino acids is remarkably reminiscent of man-made motors<sup>6</sup>.

The story behind the study of the mechanism of ATP synthesis contains many dramas (BOX 1), and the

tale is still being unravelled. In this review, we focus on the mechanism of rotary catalysis of ATP synthase — that is, how rotation and catalysis are coupled and regulated in the working enzyme.

## $F_1$ and $F_0$ are both rotary motors

ATP synthase is a large protein complex (~500 kDa) with a complicated structure. It is composed of a membrane-embedded portion,  $F_0$  (read as ‘ef oh’), central and side stalks, and a large headpiece (FIG. 2). The central portion ( $F_1\gamma\epsilon$ - $F_0c_{10-14}$ ) rotates relative to the surrounding portion ( $F_1\alpha_3\beta_3\delta$ - $F_0ab_2$ ) and, for convenience, we will call the former the ‘rotor’ and the latter the ‘stator’, although the rotor–stator relationship is relative. When the magnitude of  $\Delta\bar{\mu}_{H^+}$  is large, as in functional mitochondria, downhill proton flow through  $F_0$  causes rotation of the  $F_0$  rotor and, hence, rotation of the  $\gamma\epsilon$ -subunits of  $F_1$ . The rotary motion of the  $\gamma$  alternates the structure of the  $\beta$ -subunit so that ATP is synthesized.

In the reverse reaction, ATP hydrolysis in  $F_1$  induces the rotation of  $\gamma$  and, hence, of the  $F_0$  rotor in the reverse direction. This then drives proton pumping. In either case, the side stalk connecting the stator of  $F_0$  and that of  $F_1$  prevents them being dragged by the central rotor. It is therefore possible to define the ATP synthase as a complex of two motors — an ATP-driven  $F_1$  motor and a proton-driven  $F_0$  motor. They are connected by a common rotary shaft and their genuine directions of rotation are opposite. The motor motions have been visualized for  $F_1$ , as described below and in REF. 7, but this has yet to be done for  $F_0$  (REF. 8).

Chemical Resources  
Laboratory, Tokyo  
Institute of Technology,  
Nagatsuta 4259,  
Yokohama 226-8503, Japan.  
Correspondence to M.Y.  
e-mail:  
myoshida@res.titech.ac.jp

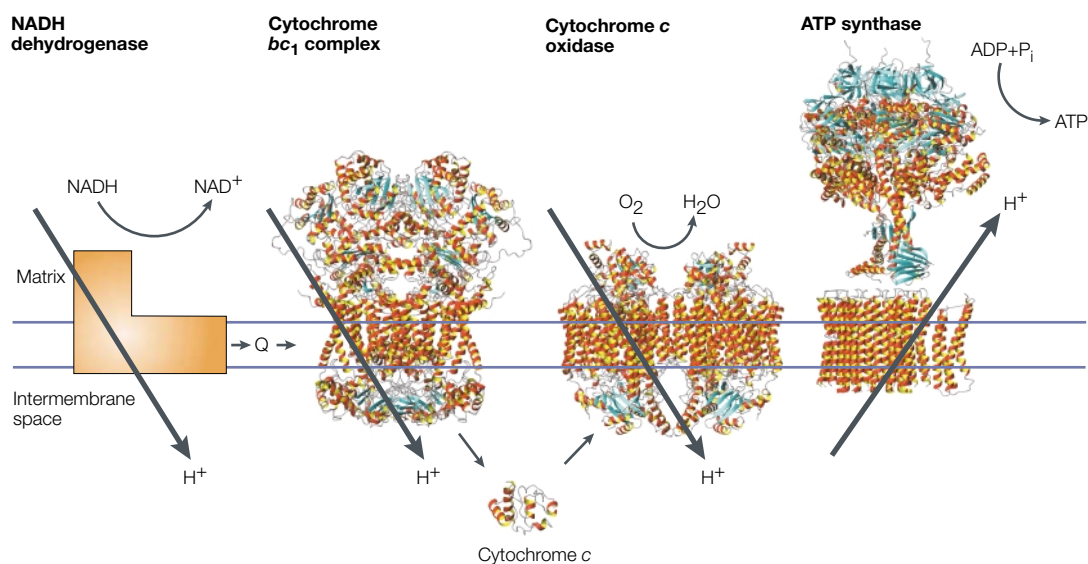


Figure 1 | **The respiratory chain and ATP synthase.** Electrons are transferred from NADH dehydrogenase to cytochrome *c* oxidase by coenzyme Q (Q), cytochrome *bc*<sub>1</sub> complex and cytochrome *c*. The established proton gradient across the inner mitochondrial membrane drives the proton flow in ATP synthase that accompanies ATP synthesis. Structures are taken from: cytochrome *bc*<sub>1</sub> complex<sup>71</sup>; cytochrome *c* oxidase<sup>72</sup>; the F<sub>1</sub> part of ATP synthase<sup>52</sup>; and the F<sub>0</sub> part of ATP synthase<sup>29</sup>.

### Structure of F<sub>1</sub>

In the initial crystal structure of the  $(\alpha\beta)_3\gamma$ -portion of native bovine mitochondrial F<sub>1</sub> (termed the 'native' structure)<sup>6</sup>, three  $\alpha$ -subunits and three  $\beta$ -subunits are arranged alternately, forming a cylinder of  $(\alpha\beta)_3$  around the coiled-coil structure of the  $\gamma$ -subunit (FIG. 3a,b). The  $\alpha$ - and  $\beta$ -subunits have a similar fold, as would be expected from their sequence similarity. All of the  $\alpha$ -subunits are bound to the ATP analogue AMP-PNP, and the three subunits adopt very similar conformations. The three  $\beta$ -subunits, however, are in three nucleotide-bound states: the first, termed  $\beta_{TP}$ , has AMP-PNP in the catalytic site (FIG. 3c); the second ( $\beta_{DP}$ ) has ADP; and the third ( $\beta_E$ ) has no bound nucleotide (FIG. 3c-e). So, the native structure of F<sub>1</sub> looks like a snapshot of the working rotary engine, with three reaction chambers representing the moment just after exhaust and intake ( $\beta_E$ ), ignition ( $\beta_{DP}$ ) and compression ( $\beta_{TP}$ ) (BOX 2). The lower part of the slightly bowing, asymmetric coiled-coil structure of the  $\gamma$ -subunit is displaced towards the  $\beta_E$ , forcing the carboxy-terminal domain of this  $\beta$ -subunit to swing  $\sim 30^\circ$  downwards. Thus, the  $\beta_E$  adopts the 'open' (O) form, whereas  $\beta_{TP}$  and  $\beta_{DP}$  have the 'closed' (C) form.

A novel crystal structure of bovine F<sub>1</sub>, with all three catalytic sites occupied by nucleotides, was recently reported<sup>9</sup>. Crystals were grown in Mg-ADP and aluminium fluoride (AlF<sub>4</sub><sup>-</sup>; a dummy phosphate inhibitor that is expected to stabilize the conformations of a catalytic transition state). In this latest structure — termed (ADP·AlF<sub>4</sub><sup>-</sup>)<sub>3</sub>F<sub>1</sub> — the two  $\beta$ s, which are identified as being equivalent to  $\beta_{TP}$  and  $\beta_{DP}$  in the native structure from their relative positions to the asymmetric  $\gamma$ -subunit, hold Mg-ADP·AlF<sub>4</sub><sup>-</sup> at their catalytic sites. Their structures are very similar to each other and to their

equivalents in the native structure. The  $\beta$ -subunit equivalent to  $\beta_E$  takes a 'half-closed' (C') conformation (FIG. 3d), and retains Mg-ADP and sulphate (a mimic of phosphate) at the catalytic site. In the C'-form  $\beta$ , the carboxy-terminal domain of the  $\beta_E$  swings  $\sim 23^\circ$  upwards, and the distance between the  $\beta$ -phosphate of ADP and the sulphate would be too long to resynthesize ATP, even if sulphate were replaced by phosphate. The coiled-coil region of the  $\gamma$ -subunit twists  $\sim 20^\circ$  in the region surrounded by the  $(\alpha\beta)_3$  cylinder and  $\sim 10^\circ$  in the region protruding from the  $(\alpha\beta)_3$  cylinder.

### Visualizing the rotation of F<sub>1</sub>

ATP-driven rotation of the  $\gamma$ -subunit in the  $(\alpha\beta)_3$  cylinder of F<sub>1</sub> has been visualized using the  $(\alpha\beta)_3\gamma$ -subcomplex from a thermophilic bacterium with three microprobes (FIG. 4). With reference to the crystal structure, the direction of the  $\gamma$ -rotation is such that one  $\beta$  undergoes a transition in the order  $\beta_{TP}$ ,  $\beta_{DP}$  and  $\beta_E$ , consistent with ATP-hydrolysis-driven rotation. At very low concentrations of ATP, rotation occurs in discrete  $120^\circ$  steps, each driven by an ATP molecule that arrives at F<sub>1</sub>. Distribution of the dwelling time (a period between one  $120^\circ$  step and the next) obeys an exponential decrease, confirming that one ATP is consumed per  $120^\circ$  step<sup>10</sup>.

Long actin filaments (FIG. 4) rotate slowly and short ones rotate more rapidly, but the torque of rotary motion, calculated from the rotational velocity of an actin filament and the frictional resistance of water (viscous load), always reached  $\sim 40$  pN nm<sup>-1</sup>. The energy required to produce this magnitude of torque is  $\sim 8 \times 10^{-20}$  J per  $120^\circ$  rotation; the free energy liberated from one molecule of ATP under the same conditions is  $\sim 9 \times 10^{-20}$  J. So the efficiency of converting the energy of ATP hydrolysis into that of rotation seems to be very high —

## SWITCH II REGION

The  $\beta$ -subunit of  $F_1$  has a region that is topologically equivalent to the switch II region of guanine-nucleotide binding (G) proteins, which changes the conformation in response to the interconversion of GTP and GDP.

around 90% (REF. 10). Lower values (50–80%) have been reported on the basis of the rotation velocity of nickel bars attached to the  $\gamma$ -subunit<sup>11</sup>. Strictly speaking, a thermodynamically accurate efficiency of energy conversion requires the measurement of work taken out of the system (such as deflection of a laser trap), rather than rotation of a filament, which dissipates energy into the medium as heat<sup>12</sup>.

$120^\circ = 90^\circ(\text{ATP on}) + 30^\circ(\text{ADP/P}_i \text{ off})$ . When an actin filament is used as a rotation marker, the viscous load imposes an artificial limit on rotation (maximum 6–8 revolutions per second (rps)). A small gold bead (diameter 40 nm) obliquely attached to the  $\gamma$ -subunit, however, is not an impeding load, so is well suited for moni-

toring rapid rotation. Rotation is detected by light scattering of a laser beam and recorded by a video with 8,000 frames per second. Rapid monitoring of rotation thus attained has revealed insights into the mechanism of rotational catalysis by  $F_1$  (REF. 13).

First, at high concentrations of ATP, a bead rotates at around 130 rps, consistent with a maximum rate of ATP hydrolysis ( $\sim 300 \text{ s}^{-1}$ ; that is, about 100 rps). The velocities of rotation at ATP concentrations from 20 nM to 2 mM agree fairly well with those expected from the rates of ATP hydrolysis of free  $F_1$  in the solution and obey simple Michaelis–Menten kinetics, with 15  $\mu\text{M}$  being an ATP concentration that gives half-maximal rotation velocity. This indicates that it might not be necessary to assume a gear change mechanism as the ATP concentration varies in the range  $>20 \text{ nM}$ .

Second, the  $120^\circ$  step of rotation is further split into  $90^\circ$  and  $30^\circ$  sub-steps. Rotation velocities of the  $90^\circ$  and  $30^\circ$  sub-steps are very fast ( $<0.1 \text{ ms}$ ). Dwelling times between a  $30^\circ$  and a subsequent  $90^\circ$  sub-step become shorter as the concentration of ATP increases and finally disappear beyond the detection limit, indicating that the  $90^\circ$  rotation is triggered by binding of a single ATP to  $F_1$  (but not by any subsequent catalytic event with a lifetime longer than 0.1 ms).

And last, dwelling times between a  $90^\circ$  and a subsequent  $30^\circ$  sub-step are always  $\sim 2 \text{ ms}$  on average at all ATP concentrations. Analyses of dwelling-time distribution indicate that at least two events, each  $\sim 1 \text{ ms}$  in length, occur sequentially in  $F_1$ . These events are most likely to be hydrolysis of a bound ATP (or the conformational transition necessary for hydrolysis of ATP), and release of the last remaining hydrolysis product, ADP or  $\text{P}_i$ . This second event triggers the  $30^\circ$  rotation, and  $F_1$  is reset for the next round of catalysis. The physical events — the binding and release of substrate and product — are coupled with the power generation, just as Boyer predicted.

**Open–closed motion of  $\beta$ s.** The  $\beta$ -subunit in  $F_1$  can take one of at least three forms — open (O), half-closed ( $C'$ ) or closed (C) (FIG. 3c–e). Altering the contact with the asymmetric  $\gamma$ -subunit in  $F_1$  will lead to a transition between these forms. Also, local changes of bound-nucleotide states at catalytic sites are amplified to the global open–closed transition of the  $\beta$ s. The isolated  $\beta$ -subunit takes the O form in the crystal structure (K. Miki and M.Y., unpublished observations), and it transforms to another conformation — most likely the C form — on binding nucleotide<sup>14</sup>. The O form  $\beta$  can readily accept ATP with ‘zipping’ of bonds between ATP and the catalytic sites, so that the open catalytic site is closed.

A comparison of the structures of the native structure ( $\beta$ s are in the CCO state) and  $(\text{ADP}\cdot\text{AlF}_4^-)_2 F_1$  structure (CCC' state) further suggests that when ATP is hydrolysed on the C-form  $\beta$ -subunit of  $F_1$ , the phosphate generated is dislocated 3.5–4 Å from the previous  $\gamma$ -phosphate position of ATP, and seems to push up the loop in the SWITCH II REGION. This, and other rearrangements of nearby residues, causes partial separation of

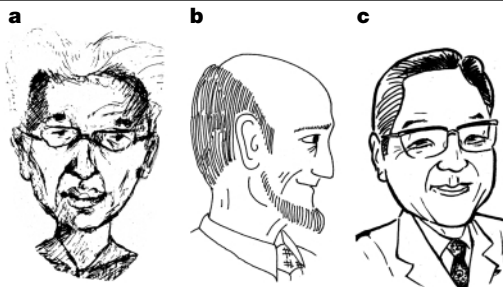
## Box 1 | A brief history of research into ATP synthase

The molecular study of ATP synthase was initiated in 1960 when Efraim Racker (a) and his colleagues reported the isolation of a soluble factor from beef heart mitochondria. The factor,  $F_1$ , had ATP hydrolysis activity<sup>61</sup> and could restore ATP synthesis in membrane fractions that had lost this activity<sup>62</sup>. They also isolated a similar factor from chloroplasts, showing that the essential features of ATP synthesis in mitochondria and chloroplasts were the same. Since then, there have been at least two notable revolutions in the study of ATP synthase.

In 1961 (REF. 2), Peter Mitchell (a Nobel laureate of 1978 (REF. 63)) proposed the chemiosmotic hypothesis, in which a long-sought high-energy chemical intermediate that would connect the oxidation of respiratory fuel and ATP synthesis was declared to be an illusion. Instead, a high-energy state — the electrochemical potential of protons across a membrane  $\Delta\bar{\mu}_{\text{H}^+}$  — was postulated. Accordingly, the putative ATP synthase was predicted to be a proton-translocating ATP synthase/hydrolyase. This hypothesis was unfamiliar and very unpopular with biochemists of the time. But the situation was changed markedly in 1966 by Andre Jagendorf’s (b) ‘acid–base transition’ experiment<sup>64</sup>. He imposed a pH gradient across chloroplast membranes and observed ATP synthesis in the absence of light. The chemiosmotic mechanism was finally established by experiments using the vesicle-reconstitution method initiated by Yasuo Kagawa (c)<sup>65</sup>. Driven by an artificially imposed  $\Delta\bar{\mu}_{\text{H}^+}$ , vesicles containing purified ATP synthase catalysed ATP synthesis<sup>66</sup>.

The next challenge was to discover how ATP synthase exchanges the energy of proton flow at  $F_0$  and ATP synthesis/hydrolysis at  $F_1$ . On the basis of the kinetics of enzyme-catalysed  $^{18}\text{O}$  exchange between  $\text{H}_2\text{O}$  and  $\text{P}_i/\text{ATP}$ , Paul Boyer (a Nobel laureate of 1997 (REF. 67)) proposed the ‘binding change’ mechanism in 1977 (REFS 17,18). According to this mechanism, each of three catalytic  $\beta$ -subunits in ATP synthase alternates sequentially between states with different affinities to nucleotides. This binding affinity change — but not chemical conversion of ATP hydrolysis/synthesis — is coupled with energy input/output. Boyer further assumed physical rotation of the centrally located  $\gamma$ -subunit as a cause of sequential change<sup>18</sup>.

Although the unusual cooperative kinetics of the enzyme (negative for ATP binding and positive for catalysis) supports the binding-change mechanism<sup>68</sup>, the idea of the rotation was so novel that there were few serious attempts to test it until over a decade later, when John Walker (a Nobel laureate of 1997 (REF. 69)) and colleagues showed how the structure of bovine  $F_1$  justified Boyer’s prediction<sup>6</sup>. Once the rotation was considered to be plausible, it took only another three years to demonstrate it — ATP-dependent crosslinking exchange experiments came first<sup>70</sup>, and then direct visualization of rotation of an actin filament attached to the  $\gamma$ -subunit swept away scepticism<sup>7</sup>.



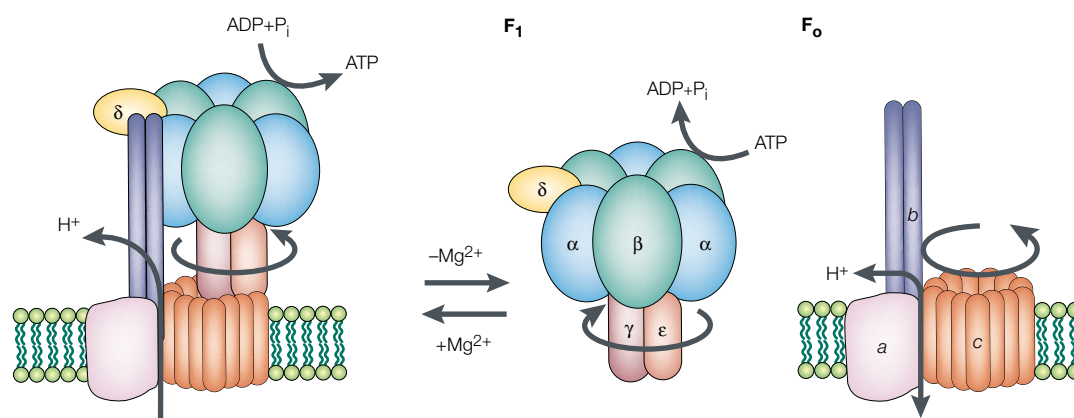


**Figure 2 | Structure of ATP synthase.** The bacterial ATP synthase is illustrated as the simplest version of ATP synthases. It is composed of a water-soluble protein complex of ~380 kDa,  $F_1$ , and a hydrophobic transmembrane portion,  $F_0$ . Removal of  $Mg^{2+}$  at low concentrations of salt allows the  $F_1$  part to be extracted in water, leaving the  $F_0$  portion in the membrane.  $F_0$  and  $F_1$  can, however, reassemble into the intact ATP synthase by adding back  $Mg^{2+}$  (REFS 61,73,74). This reversible separation of  $F_0$  and  $F_1$  has benefited study in this field.  $F_0$  acts as a proton channel by itself, and isolated  $F_1$  — often called the  $F_1$ -ATPase — catalyses ATP hydrolysis (which is considered a reverse reaction of ATP synthesis). The subunit structures of ATP synthases are well conserved during evolution, but there are some variations among sources. The simplest is bacterial ATP synthase, in which  $F_1$  contains five kinds of subunit with a stoichiometry  $\alpha_3\beta_3\gamma_1\delta_1\epsilon_1$  and  $F_0$  contains three kinds of transmembrane subunit with a stoichiometry  $a_1b_2c_{10-14}$ . The numbers of transmembrane helices are five ( $F_0a$ ), one ( $F_0b$ ) and two ( $F_0c$ ). Chloroplast ATP synthase has the same subunit composition except that two kinds of  $F_0b$  homologue exist. Mitochondrial ATP synthase has at least six kinds of additional accessory subunit. Confusing subunit nomenclature remains for historical reasons (for example, mitochondrial  $\delta$  corresponds to bacterial  $\epsilon$ , and the mitochondrial subunit named OSCP corresponds to bacterial  $\delta$ ), but in this review we use the names of subunits according to the bacterial enzyme. The catalytic sites for ATP hydrolysis are located on the  $\beta$ -subunits of  $F_1$ , but residues of the  $\alpha$ -subunits also contribute. The  $\alpha$ -subunits contain a non-catalytic nucleotide-binding site, the function of which is not yet fully understood. The central stalk is made of the  $\gamma$ - and  $\epsilon$ -subunits, and the side stalk from the  $F_1\delta$ - and  $F_0b_2$ -subunits.

the two  $\beta$ -strands (one before the P-LOOP and the other before the switch II loop), which leads to the outward (opening) movement of the whole carboxy-terminal domain of  $\beta$ . This movement produces the C' form, and subsequent loss of ADP/ $P_i$  from the catalytic site sets the conformation of the  $\beta$ -subunit to the O form.

The open–closed state of each  $\beta$  in  $F_1$  is thus decided by its bound-nucleotide state and by the orientation of  $\gamma$ . This means that the nucleotide states of  $\beta$ s in  $F_1$  can determine the orientation of the  $\gamma$ -subunit and vice versa; the latter determines the former. The alternating, sequential ATP hydrolysis accompanies the coordinated open–closed motion of  $\beta$ s and thereby rotation of the  $\gamma$ -subunit. Conversely, if the  $\gamma$ -subunit is forced to rotate by the  $F_0$  motor, this can induce changes in the nucleotide-binding states of the  $\beta$ -subunits, resulting in the synthesis of ATP. Indeed, the dynamic occurrence of the CCO (or CCC') state during catalytic turnover has been shown by the formation of a specific crosslink that can bridge only between two C-form  $\beta$ -subunits in an  $F_1$  molecule<sup>15</sup>, and the activity of  $F_1$  is lost by fixing the  $\beta$ -subunits in the C form<sup>16</sup>.

#### Models to account for catalysis and rotation

Boyer's classic model of rotary catalysis assumes that one or two catalytic sites are occupied by ATP (or ADP) at any moment of steady-state catalysis<sup>17,18</sup> (BOX 2). The  $(ADP\cdot AlF_4^-)_2F_1$  structure, however, favours the models by which two or three catalytic sites are filled with ATP (or ADP), as previously indicated from the ATP-induced change of tryptophan fluorescence<sup>19</sup>. Walker

and colleagues<sup>9</sup> have proposed a model by which concerted transitions — the closing of  $\beta_E$  driven by ATP binding and the opening of  $\beta_{DP}$  driven by ATP hydrolysis — induce the 120° rotation of the  $\gamma$ -subunit. A similar model was postulated previously by Ren and Allison<sup>20</sup>.

The latest evidence of the 90°–30° sub-steps, as well as the  $(ADP\cdot AlF_4^-)_2F_1$  structure, lead us to propose a model to explain the catalysis–rotation relationship (FIG. 5). Details can be found in the figure legend, but three main points are worth mentioning here. First, the  $\gamma$ -subunit in the  $(ADP\cdot AlF_4^-)_2F_1$  structure has a ~20° clockwise twist (viewed from the membrane side) at the middle part compared with the native structure. So, the ADP/ $P_i$  release from the C'-form  $\beta$  (CCC' → CCO) probably induces a relaxation of this torsion; that is, a ~20° anticlockwise rotation, which probably corresponds to the observed 30° sub-step.

Second, as pointed out by Walker and colleagues, when one  $\beta$ -subunit takes the C' form, another  $\beta$ -subunit (located at the anticlockwise side, viewed from the membrane side) might adopt a catalytically active C form (denoted  $C_A$ ), which mediates reversible cleavage of the  $\gamma$ -phosphate of ATP. Last, this model can explain why ATP synthase binds ADP and  $P_i$  preferentially in the presence of excess ATP in the ATP-synthesis reaction — proton flow through  $F_0$  drives the ~30° rotation of the  $\gamma$ -subunit, turning the empty O-form  $\beta$  to the empty C'-form  $\beta$  that can accept only ADP and  $P_i$ . Without ADP and  $P_i$ , the empty C'-form  $\beta$  is not filled and ATP synthesis would stop at this point. Consistent

#### P-LOOP

Various ATP-metabolizing proteins contain a consensus sequence Gly-X-X-Gly-X-Gly-Lys-Thr (X is variable). This sequence is found in a loop connecting a  $\beta$ -strand (adjacent to a  $\beta$ -strand of switch II region) and an  $\alpha$ -helix. The lysine and threonine residues in the P-loop are recruited for binding the phosphate moiety of nucleotides.

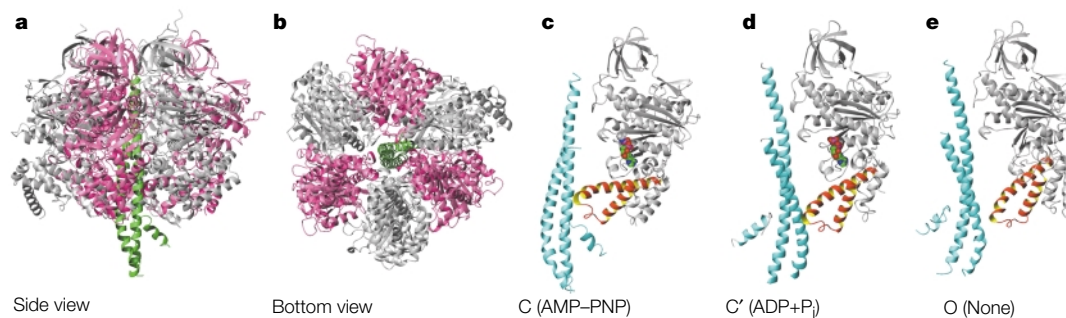


**Figure 3 | The crystal structure of mitochondrial  $F_1$ -ATPase.** Side view (**a**) and view from the bottom (**b**) of the  $\alpha_3\beta_3\gamma$  part of bovine heart mitochondrial  $F_1$  (REF. 3). A coiled-coil structure of the  $\gamma$ -subunit penetrates the  $(\alpha\beta)_3$  cylinder. This structure apparently embodies Boyer's rotary catalysis hypothesis. **c–e** | Three conformations of  $\beta$ -subunits. The structure of the  $\gamma$ -subunit is also shown. **c** | Closed (C) form. A  $\beta$ -subunit with bound AMP–PNP ( $\beta_{TP}$ ) is shown.  $\beta$ -subunit with bound ADP ( $\beta_{DP}$ ) and the  $\alpha$ -subunits are also in the closed form. **d** | Half-closed ( $C'$ ) form. A  $\beta$ -subunit with bound ADP and sulphate (a mimic of phosphate) is shown. **e** | Open (O) form. A  $\beta$ -subunit with an empty catalytic site ( $\beta_E$ ) is shown. The carboxy-terminal helix-rich domain of the  $C'$  and O forms of  $\beta$ s swing  $\sim 23^\circ$  and  $\sim 30^\circ$  outwards, respectively, from the centre of the molecule as a rigid body. The helices of the domain are highlighted.

with this,  $\Delta\bar{\mu}_{H^+}$  alone is not enough to promote the release of product ATP from ATP synthase or to drive rotation of the  $\gamma$ -subunit; in both cases ADP and  $P_i$  are required<sup>21–23</sup>.

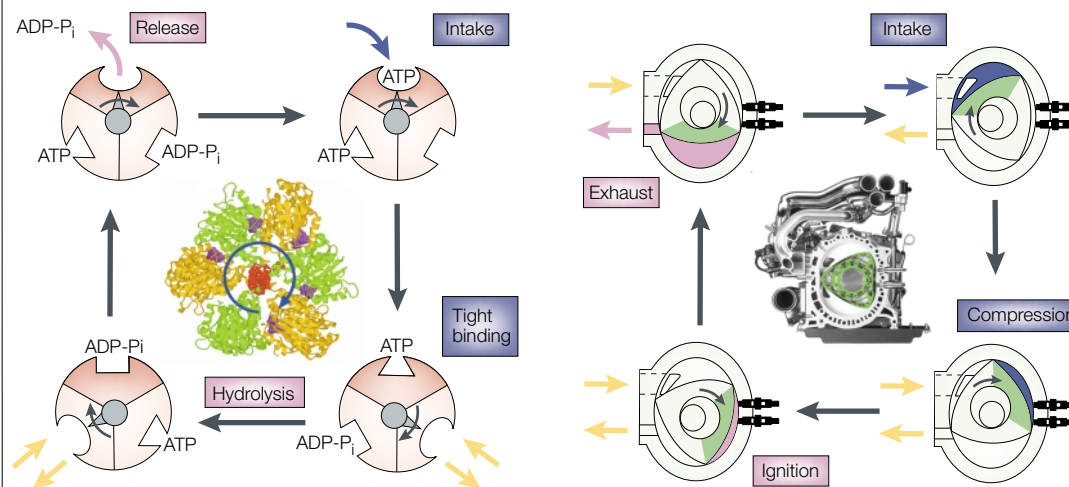
**The  $F_o c$  ring is a rotor**

Although the whole structure of the  $F_o$  part of ATP synthase is not known, the crystal structure of  $F_1F_o c_{10}$  of the yeast ATP synthase has shown that  $F_o c$ -subunits are arranged as a ring, and that the foot of the central shaft  $\gamma$  lands on — but does not penetrate into — the cyto-

plasmic surface of the ring<sup>24</sup>. It is generally thought that  $F_o a$  associates with the outside surface of the  $F_o c$  ring, and that  $F_o b_2$  associates with  $F_o a$  and  $F_1\delta$ .

The  $F_o c$  ring is a rotor. Rotation of both the  $\gamma$ -subunit and the  $F_o c$  ring by ATP has been shown by an actin filament attached to the amino termini of  $F_o c$  on the immobilized ATP synthase<sup>8,25,26</sup>. However, rotation was even observed for an enzyme with inactivated  $F_o$ , which had lost the ability to transport protons, and it turned out that subunit associations in  $F_o$  were impaired by the detergents used<sup>8</sup>. In fact, all of the  $F_o$ -

**Box 2 | Rotary engines in the car and in the cell**



The  $F_1$  motor reminds us of the rotary combustion engine, which was invented by Felix Wankel in 1957 and was first used in commercial cars by Mazda in 1967. The rotary engine is small, light, silent and simple because the engine can directly convert the fuel energy into rotation of the rotor. It can drive the intake of the fuel gas, compression, ignition and exhaust sequentially just by a simple rotation of the central rotor, which is quasi-triangular in shape (right panel). The events occurring on one side of the rotor (green) are annotated.

The  $F_1$  also has a central rotor — the  $\gamma$ -subunit — and three reaction chambers (the catalytic  $\beta$ -subunits; left panels). The events occurring in one  $\beta$ -subunit (light red) are annotated according to Boyer's classic model. The basic principles behind the functioning of these rotors — three reaction sites in turn doing each of three cyclic steps in a  $120^\circ$  phase difference to cause rotary motion — are remarkably similar.

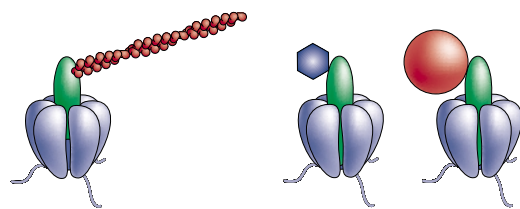


**Figure 4 | Microprobes to detect the rotation of a nanomotor.** The  $(\alpha\beta)_3$  cylinder is fixed on the glass surface and one of three kinds of rotation marker is attached to the  $\gamma$ -subunit. **a** | A fluorescently labelled actin filament (1–4  $\mu\text{m}$ )<sup>7</sup>. **b** | A single fluorescent dye (~2 nm)<sup>75</sup>. **c** | A bead (gold (40 nm) or polystyrene (0.5  $\mu\text{m}$ ))<sup>13</sup>.

subunits, with the exception of  $F_0c$ , were lost from the crystals of yeast ATP synthase formed in dodecylmalto-side<sup>24</sup>. Evidence from biochemical studies showed that ATP synthase, in which  $\gamma$ ,  $\epsilon$  and  $F_0c$  were crosslinked, retained activities of ATP synthesis and ATP-driven proton translocation<sup>27</sup>. Thus,  $\gamma$ ,  $\epsilon$  and the  $F_0c$  ring must rotate together as one body without slack. Note that the  $F_0c$  ring in ATP synthase is permanently asymmetric because the  $\gamma\epsilon$ -subunits are connected to the fixed members of  $F_0c$ -subunits in the ring. ATP-dependent subunit rotation between the  $F_0c$  ring and  $F_0a$  was supported by  $F_0c$ – $F_0a$  crosslinking experiments<sup>28</sup>.

**Symmetry mismatch between  $F_1$  and  $F_0$ .** The assumption that ATP synthase contains 12 copies of  $F_0c$ -subunits used to be generally accepted. In this case, one proton moves the  $F_0c$  ring by  $30^\circ$ , and four protons drive the  $120^\circ$  that matches one step of rotation of  $\gamma$  (proton:ATP ratio is 4). Models for the  $F_0$  motor have been proposed and discussed on this assumption<sup>29</sup>, but several recent structural studies do not support it (FIG. 6). For example, the crystal structure of a partial complex of yeast ATP synthase contains ten copies of the  $F_0c$ -subunits<sup>24</sup>. Atomic-force and electron micrographs showed 14 copies of  $F_0c$  in chloroplast ATP synthase<sup>30</sup>, and 11 copies in *Ilyobacter tartaricus* ATP synthase<sup>31</sup>. The possibility that this is an artefact arising from the deteriorating effect of the strong detergents used in these experiments (sodium dodecylsulphate) has to be kept in mind, but a recent experiment in the absence of detergents using genetically fused  $F_0c$  polymers in *E. coli* ATP synthase revised the previous stoichiometry of  $F_0c$ -subunits from 12 to 10 (REF. 32). So, the possibility is increasing that the number of copies of  $F_0c$ -subunits in the  $F_0c$  ring differ, depending on the species or even on the growth conditions, as suggested by Schmidt and colleagues<sup>33</sup>.

If this is the case, there are several serious — but interesting — consequences. The first is that the proton:ATP ratio can be non-integral and variable — analogous to the clutch plate of a car, which allows more slip than the tight toothing of two gears. Second, the rotation step of the  $\gamma$ -subunit ( $120^\circ$ ) cannot be a multiple of that of  $F_0c$  ( $36^\circ$  if 10 copies of  $F_0c$  exist), despite the fact that the  $\gamma\epsilon$ -subunits and the  $F_0c$  ring rotate together as an ensemble without displacement (as shown by a  $\gamma$ – $\epsilon$ – $F_0c$  crosslink

study<sup>27</sup>). Torque force is generated and transferred at the precisely aligned stator–rotor interfaces between the  $\gamma$ - and  $\beta$ -subunits and between the  $F_0c$ - and  $F_0a$ -subunits. However, after each step of rotation, misalignment inevitably happens to one of the contact sites and it must be adjusted to the right positions by some means. Both a side stalk,  $F_0b_2$ – $F_1\delta$  that has an extra flexibility<sup>34</sup>, and the coiled-coil structure of the  $\gamma$ -subunit that allows some internal twisting, are good candidates for the ‘absorber’ of this transient structural torsion accompanied with the adjustment.

**Electrostatic motor versus power stroke.** The mechanism of the  $F_0$  motor remains more elusive than that of the  $F_1$  motor. When a proton passes through  $F_0c$ ,  $F_0a$  exerts a sliding force on the  $F_0c$  ring without breaking its association with the ring. Therefore, two kinds of interaction or contact site, a driving unit and a rail, are assumed between the  $F_0c$  ring and  $F_0a$ . Two essential residues — proton-translocating carboxylate (aspartate or glutamate) in transmembrane helix 2 of  $F_0c$  and the conserved arginine residue in transmembrane helix 4 of  $F_0a$  — would lie closely and presumably form a proton channel. Some models propose that the change in electrostatic interactions between these two residues upon protonation/deprotonation is a key step of torque generation<sup>35,36</sup>. However, one constraint on this model is the varied arrangement of proton-translocating carboxylates seen in the V-ATPASE family, which is evolutionarily related to ATP synthase.

The proton motor of the V-ATPase is thought to have the same mechanism as that of the  $F_0$  motor. The

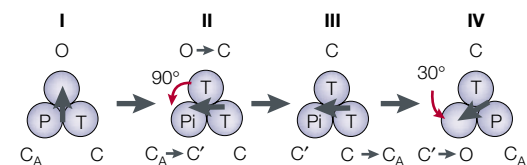


**Figure 5 | Model for the rotary catalysis of ATP synthase.**

The change of states of the three  $\beta$ -subunits and the  $\gamma$ -subunit (arrow) during hydrolysis of one ATP ( $120^\circ$  rotation) is illustrated. Starting from the CCO state (I), the sequence of events in ATP hydrolysis reaction is as follows. I→II, ATP binds to the O-form  $\beta$ , which undergoes an O→C transition. Simultaneously, the  $C_A$  form  $\beta$  undergoes a  $C_A$ → $C'$  transition and the  $\gamma$ -subunit rotates  $90^\circ$ . This process takes place within 0.1 ms. II→III, the C-form  $\beta$  undergoes a C→ $C_A$  transition. This occurs at a rate constant of  $\sim 1 \times 10^3 \text{ s}^{-1}$  (lifetime  $\sim 1$  ms). III→IV, ADP/ $P_i$  is released from the  $C'$ -form  $\beta$  which then undergoes a  $C'$ →O transition and the  $\gamma$ -subunit rotates  $30^\circ$ . This process takes place at a rate constant of  $\sim 1 \times 10^3 \text{ s}^{-1}$  (lifetime  $\sim 1$  ms). Transitions II→III and III→IV are rate-limiting steps at saturating ATP concentrations. The  $C_A$ → $C'$  transition accompanies the separation of  $P_i$  from ADP on  $F_1$ . A single  $\beta$ -subunit undergoes a sequential change of states,  $C(\text{ATP})$ → $C_A(\text{ADP}\cdot\text{P}_i)$ → $C'(\text{ADP}\cdot\text{P}_i)$ →O(empty)→C(ATP), during three catalytic turnovers of ATP hydrolysis. In ATP synthesis, the reversed order of events occurs. C, closed-form of  $\beta$ -subunit that accommodates ATP (denoted by T);  $C'$ , half-closed form of  $\beta$ -subunit that accommodates ADP and  $P_i$  (denoted by P);  $C_A$ , catalytically active closed form of  $\beta$ -subunit on which ATP and ADP· $P_i$  are interconvertible (denoted by P); O, open form of  $\beta$ -subunit with an empty catalytic site.

#### V-ATPASE

V-ATPase is responsible for ATP synthesis in archaeobacteria and a small number of eubacteria. In eukaryotic cells, it works as a proton-translocating machinery driven by ATP hydrolysis, and it is responsible for the acidification of lysosome lumens, chromaffin granules and vacuoles.

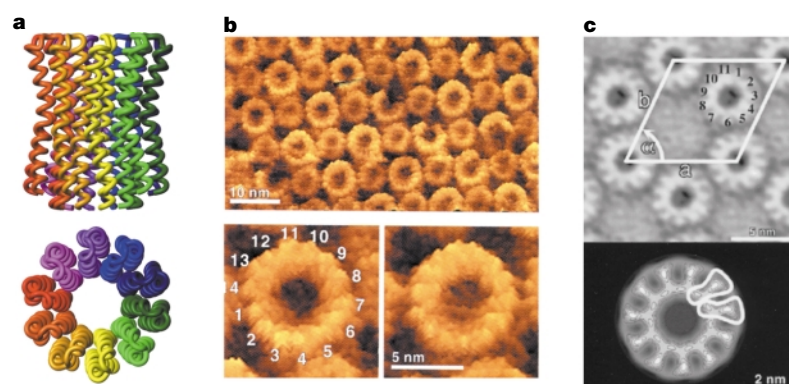


**Figure 6 | How many copies of the  $F_0c$ -subunit are in the ring?** Different numbers of  $F_0c$ -subunits in the  $F_0c$  ring have been reported. **a** | Ten copies. Crystal structure of the  $F_0c$  ring of yeast mitochondrial ATP synthase<sup>24</sup>. **b** | 14 copies. Atomic-force micrograph image of the spinach chloroplast  $F_0c$  ring<sup>30</sup>. **c** | 11 copies. Cryo-electron micrograph image of the  $F_0c$  ring from *Ilyobacter tartaricus* ATP synthase<sup>31</sup>.

$c$ -subunits of V-ATPases ( $V_0c$ ) are mostly a fused dimer form of a prototype single-hairpin structure of  $F_0c$ , but the carboxylate (Glu or Asp) essential for proton translocation is found only in the second hairpin (helix 4) in  $V_0c$ . A fused trimer form of the  $V_0c$ -subunit is also known; here, essential carboxylates are conserved in the second and third hairpins but lost in the first<sup>37</sup>. ATP synthase containing fused dimer(s) of  $F_0c$ , with the essential carboxylate being only at helix 1, has also been reported<sup>38</sup>. The variable alignment of essential carboxylates in the ring does not favour the models that assume lateral proton diffusion among the carboxylates<sup>39</sup>. An

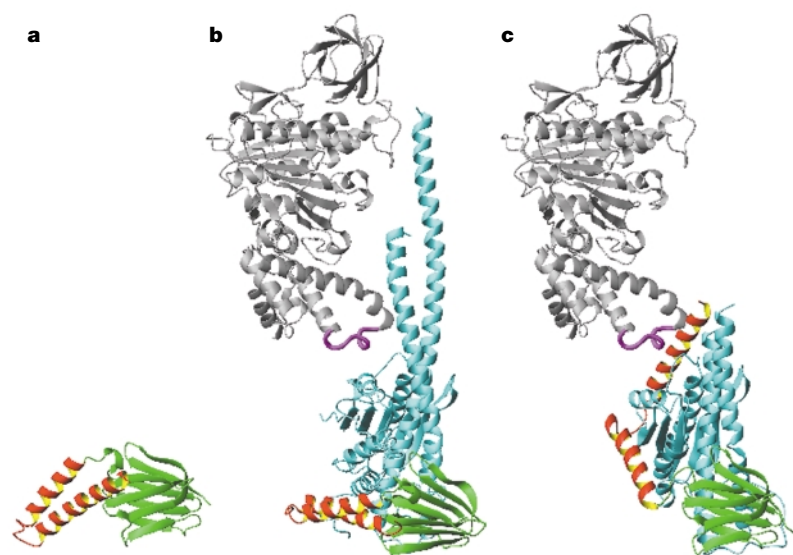


**Figure 7 | Conformational transition of the  $\epsilon$ -subunit.** **a** | Structure of the isolated  $\epsilon$ -subunit of *Escherichia coli* ATP synthase<sup>76</sup>. This is a 'down' conformation. **b** | Structure of bovine  $F_1$  (REF. 52). The  $\beta_{TP}$ -subunit is shown, but other  $\alpha$ - and  $\beta$ -subunits are omitted for simplicity. The structure of mitochondrial  $\delta$ -subunit (equivalent to the bacterial  $\epsilon$ -subunit) is similar to, if not the same as, the down conformation. **c** | Structure of the  $\epsilon$ -subunit co-crystallized with the truncated  $\gamma$ -subunit of *E. coli* ATP synthase<sup>51</sup>. Using the structure of the  $\gamma$ -subunit as a reference, the  $\beta_{TP}$ -subunit has been put into the figure. Whereas the amino-terminal  $\beta$ -barrel domain of the  $\epsilon$ -subunit (green) remains largely unchanged, the two carboxy-terminal helices (red) stand up along the  $\gamma$ -subunit and can reach the DELSEED region (violet) of the  $\beta_{TP}$ -subunit.

NMR study of monomeric *E. coli*  $F_0c$ -subunits in a water-saturated organic solvent showed that deprotonation of an essential carboxylate induced rotation of helix 2 as a unit about its axis by  $140^\circ$  (REF. 29). If this takes place in  $F_0$ , local rotations within the  $F_0c$ -subunit at the contact surface with  $F_0a$  would push the  $F_0c$  ring. This mechanism is more like a power stroke than an electrostatic motor. However,  $F_0c$  retains considerable activity when the essential carboxylate is moved from helix 2 to an opposite position of helix 1 of the hairpin structure of  $F_0c$  (D61G/A24D)<sup>40</sup>. It is not easy — but provocative — to think of a motor mechanism that allows, or even favours, variable copies of  $F_0c$  and variable arrangement of essential carboxylates in the  $c$  ring.

### Control of organellar ATP synthases

In living cells, the demand for ATP and the supply of respiration fuel (and, for photosynthetic organisms, sunshine) for the synthesis of ATP varies from one moment to the next. ATP synthase starts hydrolysing ATP as the magnitude of  $\Delta\mu_{H^+}$  becomes small, and, to prevent the wasteful consumption of ATP, the activity of ATP synthase must be suppressed.

Chloroplast ATP synthase is regulated by the formation or cleavage of a disulphide bond between two cysteine residues in a chloroplast-specific extra sequence in the  $\gamma$ -subunit. When exposed to the light, chloroplasts reduce this disulphide bond through thioredoxin, and ATP synthase is activated to synthesize ATP (REF. 41). In the dark, sulphhydryls are oxidized to form a disulphide bond, and ATP hydrolysis activity is suppressed. The peptide segment containing two cysteines can work as a transferable 'micro-switch' cassette, and its introduction into  $F_1$ s from cyanobacteria<sup>42</sup> and thermophilic bacteria<sup>43</sup> makes their ATPase activities redox-sensitive. Rotation of  $F_1$  pauses frequently when the  $\gamma$ -subunit is oxidized (D. Bald and T.H., unpublished observations).

The ATP hydrolytic activity of mitochondrial ATP synthase is inhibited by binding of a 9-kDa basic protein<sup>44</sup>. Binding depends on the presence of ATP-Mg and acidic pH; unsuitable conditions for ATP synthesis. Recent structural studies indicate that, as pH is lowered, a non-inhibitory tetramer of the protein dissociates into an inhibitory dimer, which connects two ATP synthases through their  $F_1$  portions<sup>45,46</sup>.

**Kinetic and mechanistic regulation.** In all ATP synthases from mitochondria, chloroplasts and bacteria, kinetic and mechanistic regulation is known. The catalytic turnover of ATP hydrolysis by ATP synthase and  $F_1$  is interrupted by occasional trapping of ADP-Mg at the catalytic site(s). The binding of ATP to non-catalytic nucleotide-binding sites on the  $\alpha$ -subunits facilitates the release of ADP-Mg from the affected catalytic sites, thereby recovering the ATP-hydrolysis activity<sup>47,48</sup>. At the single-molecule level, the ADP-Mg inhibition is recognized as long (~30 s) pauses of rotation (Y. Hirano-Hara and M.Y., unpublished observations). ATP synthase during steady-state ATP hydrolysis is, therefore, a dynamic mixture of the inhibited and uninhibited molecules. So, spontaneous switching of the enzyme between active

and inactive states, with a timescale much slower than the catalytic turnover, contributes to regulation. Interestingly, ATP synthesis is free from this type of inhibition<sup>49,50</sup>.

The  $\epsilon$ -subunit is an endogenous inhibitor of ATP synthase. It undergoes a drastic conformational change, with a non-inhibitory 'down' form and an inhibitory 'up' form. The carboxy-terminal  $\alpha$ -helix of the  $\epsilon$ -subunit lies on the  $F_0c$  ring in the down-form, or it is lifted up to reach the bottom of an  $(\alpha\beta)_3$ -cylinder in the up-form<sup>51–53</sup> (FIG. 7). Electrostatic interactions between basic residues in the  $\alpha$ -helix of the  $\epsilon$ -subunit and acidic residues of the conserved 'DELSEED' region of the  $\beta$ -subunit seem to stabilize the association of the  $\epsilon$ - and  $\beta$ -subunits, and the rotation is blocked<sup>54</sup>. The occupation and absence of AT(D)P at the second catalytic site facilitates up-to-down and down-to-up transitions, respectively<sup>55</sup>. The ratchet-like function of the  $\epsilon$ -subunit is intriguing; when the  $\epsilon$ -subunit is fixed in the up-form by covalent crosslinking to the  $\gamma$ -subunit, ATP-synthesis activity is maintained whereas ATP hydrolysis is blocked<sup>56</sup>.

**Unidirectional inhibition of the motor.** In nature, all enzymes catalyse both forward and reverse reactions, and it is impossible to block the reverse reaction without affecting the forward one. Therefore, the apparently unidirectional inhibition of ATP hydrolysis described above can be explained only by transformations of ATP synthase. ATP synthase somehow senses conditions favourable for ATP synthesis and transforms itself into a high-catalytic-activity form. One signal could be a large  $\Delta\bar{\mu}_{H^+}$ , and indeed, activation by  $\Delta\bar{\mu}_{H^+}$  was reported for ATP synthases from chloroplasts<sup>57</sup>, mitochondria<sup>58</sup> and bacteria<sup>59</sup>.

$\Delta\bar{\mu}_{H^+}$  is composed of  $\Delta pH$  and  $\Delta\psi$  (the electric potential difference across membranes), and an exclusive role for  $\Delta\psi$  as a signal has been proposed<sup>60</sup>. The transformation could involve the following: release of the inhibitory ADP-Mg; transition of the  $\epsilon$ -subunit to the non-inhibitory form; cleavage of a disulphide bond (chloroplast ATP synthase); and release of an inhibitor

protein (mitochondrial ATP synthase). This high-activity form of the enzyme has the potential to catalyse both hydrolysis and synthesis at high efficiency, but the thermodynamic balances allow only the net synthesis of ATP. Under conditions that are favourable for ATP hydrolysis, but not for ATP synthesis, ATP synthase drops into a low-activity form (both for ATP synthesis and hydrolysis), and ATP hydrolysis is suppressed. How the thermodynamic conditions define ATP synthase activity is yet to be clarified.

### Perspectives

ATP synthase is a splendid enzyme. But why is it so? For the purpose of proton-flow-driven ATP synthesis alone, a much simpler enzyme could have been adopted. The most challenging question is why ATP synthase needs to rotate if it is not a machine of movement. Probably related to this, the reversible separation of  $F_1$  from  $F_0$  must have a functional basis that we do not know.

The study of how ATP synthase is regulated is just beginning to come into our molecular scope and two research directions — the actual role in living cells under various conditions and the mechanisms that allow the dynamic behaviours of enzyme molecules — need to be explored.

As a motor protein, ATP synthase offers a rare research opportunity. Structures of the  $F_1$  motor, both rotor and stator in the same assembly, are known in atomic detail for the first time, and rotation can be analysed at sub-millisecond time resolution. And the atomic structure of the  $F_0$  motor is expected to be determined in the near future. An emerging possibility of step-size mismatch between the  $F_1$  and  $F_0$  motors provides an opportunity to find a novel coupling mechanism of the two motors that will explain why the mismatch is good for the enzyme. Finally, one can even dream of using this, the world's tiniest motor, as an engine part in the fabrication of nano-machines. The marvel of ATP synthase will continue.

### Links

FURTHER INFORMATION Yoshida lab | Hisabori lab

- Boyer, P. D. The ATP synthase — a splendid molecular machine. *Annu. Rev. Biochem.* **66**, 717–749 (1997). **Boyer's rotational catalysis and alternate-binding change model are concisely reviewed.**
- Mitchell, P. Coupling of phosphorylation to electron and hydrogen transfer by a chemiosmotic type mechanism. *Nature* **191**, 144–148 (1961). **This paper introduced a new concept of chemiosmotic theory into the field of bioenergetics.**
- Kanazawa, H., Kayano, T., Mabuchi, K. & Futai, M. Nucleotide sequence of the genes coding for  $\alpha$ -,  $\beta$ - and  $\gamma$ -subunits of the proton-translocating ATPase of *Escherichia coli*. *Biochem. Biophys. Res. Commun.* **103**, 604–612 (1981).
- Walker, J. E., Fearnley, I. M., Gay, N. J., Gibson, B. W. & Tybulewicz, V. L. J. Primary structure and subunit stoichiometry of  $F_1$ -ATPase from bovine mitochondria. *J. Mol. Biol.* **184**, 677–701 (1985).
- Hudson, G. S. *et al.* A gene cluster in the spinach and pea chloroplast genomes encoding one  $C\beta_1$  and three  $C\beta_2$  subunits of the H<sup>+</sup>-ATP synthase complex and the ribosomal protein S2. *J. Mol. Biol.* **196**, 283–298 (1987).
- Abrahams, J. P., Leslie, A. G., Lutter, R. & Walker, J. E. Structure at 2.8 Å of  $F_1$ -ATPase from bovine heart mitochondria. *Nature* **370**, 621–628 (1994). **The demonstration of the molecular structure of the major part of the enzyme strongly indicated the rotation of the central  $\gamma$ -subunit surrounded by the cylinder of  $\alpha_3\beta_3$ -subunits.**
- Noji, H., Yasuda, R., Yoshida, M. & Kinosita, K. J. Direct observation of the rotation of  $F_1$ -ATPase. *Nature* **386**, 299–302 (1997). **The striking direct demonstration of the rotation of the  $\gamma$ -subunit.**
- Tsunoda, S. P. *et al.* Observations of rotation within the  $F_0F_1$ -ATP synthase: deciding between rotation of the  $F_0c$  subunit ring and artifact. *FEBS Lett.* **470**, 244–248 (2000).
- Menz, R. I., Walker, J. E. & Leslie, A. G. W. Crystal structure of bovine mitochondrial  $F_1$ -ATPase with nucleotide bound to all three catalytic sites: implications for the mechanism of rotary catalysis. *Cell* **106**, 331–341 (2001). **Three bound adenine nucleotides at the catalytic sites and the slightly twisted  $\gamma$ -subunit led to the proposal of an intermediate structure during catalysis.**
- Yasuda, R., Noji, H., Kinosita, K. J. & Yoshida, M.  $F_1$ -ATPase is a highly efficient molecular motor that rotates with discrete 120° steps. *Cell* **93**, 1117–1124 (1998).
- Soong, R. K. *et al.* Powering an inorganic nanodevice with a biomolecular motor. *Science* **290**, 1555–1558 (2000).
- Oster, G. & Wang, H. Why is the efficiency of the  $F_1$  ATPase so high? *J. Bioenerg. Biomembr.* **32**, 459–469 (2000).
- Yasuda, R., Noji, H., Yoshida, M., Kinosita, K. J. & Itoh, H. Resolution of distinct rotational substeps by submillisecond kinetic analysis of  $F_1$ -ATPase. *Nature* **410**, 898–904 (2001). **A 120° step rotation is further divided into 90° and 30° substeps. ATP binding triggers the former and release of ADP•P<sub>i</sub> does the latter substep.**
- Yagi, H. *et al.* Functional conformation changes in the  $F_1$ -ATPase  $\beta$  subunit probed by 12 tyrosine residues. *Biophys. J.* **77**, 2175–2183 (1999).
- Tsunoda, S. P., Muneyuki, E., Amano, T., Yoshida, M. & Noji, H. Cross-linking of two  $\beta$  subunits in the closed conformation in  $F_1$ -ATPase. *J. Biol. Chem.* **274**, 5701–5706 (1999).
- Ren, H., Dou, C., Stelzer, M. S. & Allison, W. S. Oxidation of the  $\alpha_3(\text{BD311C/R333C})_2\gamma$  subcomplex of the thermophilic *Bacillus* PS3  $F_1$ -ATPase indicates that only two  $\beta$ -subunits can exist in the closed conformation

- simultaneously. *J. Biol. Chem.* **274**, 31366–31372 (1999).
17. Kaylor, C., Rosing, J. A. N. & Boyer, P. D. An alternating site sequence for oxidative phosphorylation suggested by measurement of substrate binding patterns and exchange reaction inhibitions. *J. Biol. Chem.* **252**, 2486–2491 (1977).
  18. Gresser, M. J., Myers, J. A. & Boyer, P. D. Catalytic site cooperativity of beef heart mitochondrial F<sub>1</sub> adenosine triphosphatase. Correlations of initial velocity, bound intermediate, and oxygen exchange measurements with an alternating three-site model. *J. Biol. Chem.* **257**, 12030–12038 (1982).
  19. Weber, J., Wilke-Mounts, S., Lee, R. S. F., Grell, E. & Senior, A. E. Specific placement of tryptophan in the catalytic sites of *Escherichia coli* F<sub>1</sub>-ATPase provides a direct probe of nucleotide binding: maximal ATP hydrolysis occurs with three sites occupied. *J. Biol. Chem.* **268**, 20126–20133 (1993).
  20. Ren, H. & Allison, W. S. On what makes the  $\gamma$ -subunit spin during ATP hydrolysis by F<sub>1</sub>. *Biochim. Biophys. Acta* **1458**, 221–233 (2000).
  21. Hackney, D. D., Rosen, G. & Boyer, P. D. Subunit interaction during catalysis: alternating site cooperativity in photophosphorylation shown by substrate modulation of [<sup>18</sup>O]ATP species formation. *Proc. Natl Acad. Sci. USA* **76**, 3646–3650 (1979).
  22. Hackney, D. D. & Boyer, P. D. Subunit interaction during catalysis. Implications of concentration dependency of oxygen exchanges accompanying oxidative phosphorylation for alternating site cooperativity. *J. Biol. Chem.* **253**, 3164–3170 (1978).
  23. Zhou, Y., Duncan, T. M. & Cross, R. L. Subunit rotation in *Escherichia coli* F<sub>1</sub>F<sub>0</sub>-ATP synthase during oxidative phosphorylation. *Proc. Natl Acad. Sci. USA* **94**, 10583–10587 (1997).
  24. Stock, D., Leslie, A. G. W. & Walker, J. E. Molecular architecture of the rotary motor in ATP synthase. *Science* **286**, 1700–1705 (1999).
  25. Sambongi, Y. *et al.* Mechanical rotation of the c subunit oligomer in ATP synthase (F<sub>0</sub>F<sub>1</sub>): direct observation. *Science* **286**, 1722–1724 (1999).
  26. Pänke, C., Gumbiowski, K., Junge, W. & Engelbrecht, S. F<sub>1</sub>-ATPase: specific observation of the rotating c subunit oligomer of EF<sub>1</sub>F<sub>0</sub>. *FEBS Lett.* **472**, 34–38 (2000).
  27. Tsunoda, S. P., Aggeler, R., Yoshida, M. & Capaldi, R. A. Rotation of the c subunit oligomer in fully functional F<sub>1</sub>F<sub>0</sub> ATP synthase. *Proc. Natl Acad. Sci. USA* **98**, 898–902 (2001).
  28. Hutcheon, M. L., Duncan, T. M., Ngai, H. & Cross, R. L. Energy-driven subunit rotation at the interface between subunit a and the c oligomer in the F<sub>0</sub> sector of *Escherichia coli* ATP synthase. *Proc. Natl Acad. Sci. USA* **98**, 8519–8524 (2001).
  29. Rastogi, V. K. & Girvin, M. K. Structural changes linked to proton translocation by subunit c of the ATP synthase. *Nature* **402**, 263–268 (1999).
  30. Seelert, H. *et al.* Structural biology. Proton-powered turbine of a plant motor. *Nature* **405**, 418–419 (2000).
  31. Stahlberg, H. *et al.* Bacterial Na<sup>+</sup>-ATP synthase has an undecameric rotor. *EMBO Rep.* **2**, 229–233 (2001).
  32. Jiang, W., Hermolin, J. & Fillingame, R. H. The preferred stoichiometry of c subunits in the rotary motor sector of *Escherichia coli* ATP synthase is 10. *Proc. Natl Acad. Sci. USA* **98**, 4966–4971 (2001).
  33. Schemidt, R. A., Qu, J., Williams, J. R. & Brusilow, W. S. Effects of carbon source on expression of F<sub>0</sub> genes and on the stoichiometry of the c subunit in the F<sub>1</sub>F<sub>0</sub> ATPase of *Escherichia coli*. *J. Bacteriol.* **180**, 3205–3208 (1998).
  34. Sorgen, P. L., Bubb, M. R. & Cain, B. D. Lengthening the second stalk of F<sub>1</sub>F<sub>0</sub> ATP synthase in *Escherichia coli*. *J. Biol. Chem.* **274**, 36261–36266 (1999).
  35. Elston, T., Wang, H. & Oster, G. Energy transduction in ATP synthase. *Nature* **391**, 510–513 (1998).
  36. Dimroth, P., Wang, H., Grabe, M. & Oster, G. Energy transduction in the sodium F<sub>1</sub>F<sub>0</sub> ATPase of *Propionigenium modestum*. *Proc. Natl Acad. Sci. USA* **96**, 4924–4929 (1999).
  37. Ruppert, C. *et al.* The proteolipid of the A<sub>0</sub>A<sub>3</sub> ATP synthase from *Methanococcus jannaschii* has six predicted transmembrane helices but only two proton-translocating carboxyl groups. *J. Biol. Chem.* **274**, 25281–25284 (1999).
  38. Aurfurth, S., Schagger, H. & Muller, V. Identification of subunits a, b, and c1 from *Acetobacterium woodii* Na<sup>+</sup>-F<sub>1</sub>F<sub>0</sub>-ATPase. Subunits c1, c2, and c3 constitute a mixed c-oligomer. *J. Biol. Chem.* **275**, 33297–33301 (2000).
  39. Junge, W., Lill, H. & Engelbrecht, S. ATP synthase: an electrochemical transducer with rotatory mechanics. *Trends Biochem. Sci.* **22**, 420–423 (1997).
  40. Miller, M. J., Oldenburg, M. & Fillingame, R. H. The essential carboxyl group in subunit c of F<sub>1</sub>F<sub>0</sub> ATP synthase can be moved and H<sup>+</sup>-translocating function retained. *Proc. Natl Acad. Sci. USA* **87**, 4900–4904 (1990).
  41. Nalin, C. M. & McCarty, R. E. Role of a disulfide bond in the  $\gamma$ -subunit in activation of the ATPase of chloroplast coupling factor 1. *J. Biol. Chem.* **259**, 7275–7280 (1984).
  42. Werener-Gruene, S., Gunkel, D., Schumann, J. & Strotmann, H. Insertion of a chloroplast-like regulatory segment responsible for thiol modulation into  $\gamma$ -subunit of F<sub>1</sub>F<sub>0</sub>-ATPase of the cyanobacterium *Synechocystis* 6803 by mutagenesis of atpC. *Mol. Gen. Genet.* **244**, 144–150 (1994).
  43. Bald, D., Noji, H., Stumpp, M. T., Yoshida, M. & Hisabori, T. ATPase activity of a highly stable  $\alpha_3\beta_3\gamma$  subcomplex of thermophilic F<sub>1</sub> can be regulated by the introduced regulatory region of  $\gamma$ -subunit of chloroplast F<sub>1</sub>. *J. Biol. Chem.* **275**, 12757–12762 (2000).
  44. Lebowitz, M. S. & Pedersen, P. L. Protein inhibitor of mitochondrial ATP synthase: relationship of inhibitor structure to pH-dependent regulation. *Arch. Biochem. Biophys.* **330**, 342–354 (1996).
  45. Cabezon, E., Arechaga, I., Jonathan, P., Butler, G. & Walker, J. E. Dimerization of bovine F<sub>1</sub>-ATPase by binding the inhibitor protein, IF<sub>1</sub>. *J. Biol. Chem.* **275**, 28353–28355 (2000).
  46. Cabezon, E., Butler, P. J., Runswick, M. J. & Walker, J. E. Modulation of the oligomerization state of the bovine F<sub>1</sub>-ATPase inhibitor protein, IF<sub>1</sub>, by pH. *J. Biol. Chem.* **275**, 25460–25464 (2000).
  47. Jault, J. M. & Allison, W. S. Slow binding of ATP to noncatalytic nucleotide binding sites which accelerate catalysis is responsible for apparent negative cooperativity exhibited by the bovine mitochondrial F<sub>1</sub>-ATPase. *J. Biol. Chem.* **268**, 1558–1566 (1993).
  48. Matsui, T. *et al.* Catalytic activity of the  $\alpha_3\beta_3\gamma$  complex of F<sub>1</sub>-ATPase without noncatalytic nucleotide binding site. *J. Biol. Chem.* **272**, 8215–8221 (1997).
  49. Minkov, I. B., Vasilyeva, E. A., Fitin, A. F. & Vinogradov, A. D. Differential effects of ADP on ATPase and oxidative phosphorylation in submitochondrial particles. *Biochem. Int.* **1**, 478–485 (1980).
  50. Bald, D. *et al.* ATP synthesis by F<sub>1</sub>F<sub>0</sub>-ATP synthase independent of noncatalytic nucleotide binding sites and insensitive to azide inhibition. *J. Biol. Chem.* **273**, 865–870 (1998).
  51. Rodgers, A. J. & Wilce, M. C. Structure of the  $\gamma$ - $\epsilon$  complex of ATP synthase. *Nature Struct. Biol.* **7**, 1051–1054 (2000).
  52. Gibbons, C., Montgomery, M. G., Leslie, A. G. & Walker, J. E. The structure of the central stalk in bovine F<sub>1</sub>-ATPase at 2.4-Å resolution. *Nature Struct. Biol.* **7**, 1055–1061 (2000).
  53. Wilkens, S. & Capaldi, R. A. Solution structure of the  $\epsilon$ -subunit of the F<sub>1</sub>-ATPase from *Escherichia coli* and interactions of this subunit with  $\beta$ -subunits in the complex. *J. Biol. Chem.* **273**, 26645–26651 (1998).
  54. Hara, K. Y., Kato-Yamada, Y., Kikuchi, Y., Hisabori, T. & Yoshida, M. The role of the  $\beta$ DELSEED motif of F<sub>1</sub>-ATPase; propagation of the inhibitory effect of the  $\epsilon$ -subunit. *J. Biol. Chem.* **28**, 23969–23973 (2001).
  55. Kato-Yamada, Y., Yoshida, M. & Hisabori, T. Movement of the helical domain of the  $\epsilon$  subunit is required for the activation of thermophilic F<sub>1</sub>-ATPase. *J. Biol. Chem.* **275**, 35746–35750 (2000).
  56. Tsunoda, S. P. *et al.* Large conformational changes of the  $\epsilon$  subunit in the bacterial F<sub>1</sub>F<sub>0</sub> ATP synthase provide a ratchet action to regulate this rotary motor enzyme. *Proc. Natl Acad. Sci. USA* **98**, 6560–6564 (2001).
  57. Lohse, D. & Strotmann, H. Reaction related with  $\Delta$ pH-dependent activation of the chloroplast H<sup>+</sup>-ATPase. *Biochim. Biophys. Acta* **976**, 94–101 (1989).
  58. Galkin, M. A. & Vinogradov, A. D. Energy-dependent transformation of the catalytic activities of the mitochondrial F<sub>1</sub> × F<sub>0</sub>-ATP synthase. *FEBS Lett.* **448**, 123–126 (1999).
  59. Fischer, S., Gräber, P. & Turina, P. The activity of the ATP synthase from *Escherichia coli* is regulated by the transmembrane proton motive force. *J. Biol. Chem.* **275**, 30157–30162 (2000).
  60. Kaim, K. & Dimroth, P. ATP synthesis by F-type ATP synthase is obligatorily dependent on the transmembrane voltage. *EMBO J.* **18**, 4118–4127 (1999).
  61. Pullman, M. E., Penefsky, H. S., Datta, A. & Racker, E. Partial resolution of the enzymes catalyzing oxidative phosphorylation. I. Purification and properties of soluble, dinitrophenol-stimulated adenosine triphosphatase. *J. Biol. Chem.* **235**, 3322–3329 (1960).
  62. Penefsky, H. S., Pullman, M. E., Datta, A. & Racker, E. Partial resolution of the enzyme catalyzing oxidative phosphorylation. II. Participation of a soluble adenosine triphosphatase in oxidative phosphorylation. *J. Biol. Chem.* **235**, 3330–3336 (1960).
  63. Mitchell, P. Keilin's respiratory chain concept and its chemiosmotic consequences. *Science* **206**, 1148–1159 (1979).
  64. Jagendorf, A. T. & Uribe, E. ATP formation caused by acid-base transition of spinach chloroplasts. *Proc. Natl Acad. Sci. USA* **55**, 170–177 (1966).
- The turning point for the Mitchell's chemiosmotic theory. After this, many people began to regard the chemiosmotic theory as the strongest hypothesis for oxidative and photo-phosphorylation.**
65. Kagawa, Y. & Racker, E. Partial resolution of the enzyme catalyzing oxidative phosphorylation. XXV. Reconstitution of vesicles catalyzing <sup>32</sup>P<sub>i</sub>-adenosine triphosphate exchange. *J. Biol. Chem.* **246**, 5477–5487 (1971).
- The most convincing evidence for the chemiosmotic theory. The reconstitution method of membrane proteins described here had a profound influence over the field of membrane biochemistry.**
66. Sone, N., Yoshida, M., Hirata, H. & Kagawa, Y. Adenosine triphosphate synthesis by electrochemical proton gradient in vesicles reconstituted from purified adenosine triphosphatase and phospholipids of thermophilic bacterium. *J. Biol. Chem.* **252**, 2956–2960 (1977).
  67. Boyer, P. D. Energy, life and ATP. *Angew. Chem. Int. Ed.* **37**, 2296–2307 (1998).
  68. Grubmeyer, C., Cross, R. L. & Penefsky, H. S. Mechanism of ATP hydrolysis by beef heart mitochondrial ATPase. Rate constants for elementary steps in catalysis at a single site. *J. Biol. Chem.* **257**, 12092–12100 (1982).
  69. Walker, J. E. *ATP Synthesis by Rotary Catalysis*, 208–234 (The Nobel Foundation, Stockholm, 1997).
  70. Duncan, T. M., Bulygin, V. V., Zhou, Y., Hutcheon, M. L. & Cross, R. L. Rotation of subunits during catalysis by *Escherichia coli* F<sub>1</sub>-ATPase. *Proc. Natl Acad. Sci. USA* **92**, 10964–10968 (1995).
  71. Iwata, S. *et al.* Complete structure of the 11-subunit bovine mitochondrial cytochrome bc<sub>1</sub> complex. *Science* **281**, 64–71 (1998).
  72. Tsukihara, T. *et al.* Structures of metal sites of oxidized bovine heart cytochrome c oxidase at 2.8 Å. *Science* **269**, 1069–1074 (1995).
  73. Jagendorf, A. T. & Smith, M. Uncoupling phosphorylation in spinach chloroplasts by absence of cations. *Plant Physiol.* **37**, 135–141 (1962).
  74. Fessenden, J. M. & Racker, E. Partial resolution of the enzyme catalyzing oxidative phosphorylation. XI. Stimulation of oxidative phosphorylation by coupling factors and oligomycin; inhibition by an antibody against coupling factor 1. *J. Biol. Chem.* **241**, 2483–2489 (1966).
  75. Adachi, K. *et al.* Stepping rotation of F<sub>1</sub>-ATPase visualized through angle-resolved single-fluorophore imaging. *Proc. Natl Acad. Sci. USA* **97**, 7243–7247 (2000).
  76. Uhlin, U., Cox, G. B. & Guss, J. M. Crystal structure of the  $\epsilon$  subunit of the proton-translocating ATP synthase from *Escherichia coli*. *Structure* **5**, 1219–1230 (1997).
- Acknowledgements**  
We are grateful to A. Leslie and J. Walker for providing us with the preprint of their paper on the structure of (ADP•NF<sub>1</sub>)<sub>2</sub>F<sub>1</sub>. We also thank T. Suzuki and K. Tsukuda for their assistance in the preparation of the figures.